JOURNAL OF THERMOPHYSICS AND HEAT TRANSFER
Vol. 20, No. 2, April–June 2006

Experimental In-Cavity Radiative Calibration of High-Heat-Flux Meters

Annageri V. Murthy*
Aero-Tech, Inc., Hampton, Virginia 23666
and
Gerald T. Fraser† and David P. DeWitt‡
National Institute of Standards and Technology, Gaithersburg, Maryland 20899

The accuracy of the "in-cavity" calibration of heat-flux meters up to 500 $kW \cdot m^{-2}$ irradiance levels by insertion into the cavity of a high-temperature blackbody is examined. The experimental study consists of measurements on two thermopile heat-flux meters using two graphite-tube variable-temperature blackbodies. To provide a baseline comparison, the meters were first calibrated up to 50 $kW \cdot m^{-2}$ outside the blackbody cavity with the irradiance level determined using a well-characterized electrical substitution radiometer. In contrast to the outside calibration method, in-cavity calibration covers the full heat-flux range of the meters. The measured radiance distribution along the cavity axis, corroborated by Monte Carlo simulations, shows that the optimum location for the meter is approximately one cavity radius from the closed end of the cavity. The in-cavity measured responsivity values corrected for the effective emissivity agree with the outside-cavity values within the measurement uncertainty. The results demonstrate the feasibility of using in-cavity techniques to calibrate heat-flux meters at high irradiance levels, limited primarily by the blackbody operating temperature.

Nomenclature

d	=	diameter of the cylindrical blackbody cavity
k	=	coverage factor
L_1	=	heated length of the cylindrical blackbody cavity
L_2	=	length of the extension tube attached to the heated cavity
L_3	=	linear temperature decrease length on the extension tube
R	=	heat-flux meter responsivity
T	=	temperature
U	=	relative expanded uncertainty in the heat-flux meter responsivity
u	=	standard uncertainty of the variable
V	=	heat-flux meter output
x	=	distance from blackbody cavity base to the sensing surface of the heat-flux meter
ε	=	emissivity
ρ	=	reflectance

Subscripts

a	=	ambient conditions
b	=	cavity base
c	=	blackbody cavity
corr	=	responsivity corrected for effective emissivity and convection
cp	=	center partition of the cylindrical cavity
e	=	end of cavity heated length
eff	=	effective value
h	=	heat-flux meter holder surface
m	=	measured responsivity from the in-cavity calibration
p	=	peak value of the heat-flux meter output along the cavity axis
s	=	heat-flux meter
x	=	transfer calibration

Received 25 February 2005; revision received 31 May 2005; accepted for publication 1 June 2005; presented as Paper 2005-5323 at the AIAA 38th Thermophysics Conference, Toronto, ON, 6–9 June 2005.

*President and Consultant, 53 Sanlun Lakes Drive. Senior Member AIAA.
†Group Leader, Optical Technology Division, 100 Bureau Drive, Stop 8441.
‡Deceased.

I. Introduction

HEAT-FLUX meters widely used in aerospace and fire research applications are required to measure irradiance or heat-flux levels from 50 $kW \cdot m^{-2}$ to more than 1000 $kW \cdot m^{-2}$. Large variations in the calibration of these meters have been observed due to different calibration methods used and the difficulty in performing calibrations at high-heat-flux levels. A round-robin test sponsored by the Federal Aviation Administration[1] (FAA) between various laboratories showed variations of $\pm 8\%$ in the measured responsivity. Recently,[2] various fire laboratories in Europe and the United States conducted two sets of round-robin calibrations involving four different heat-flux meters. The measured responsivities of the meters between the different laboratories showed variations of similar magnitude as in the FAA round-robin test. A coordinated effort has been in progress to establish traceable heat-flux meter calibrations at national[3] and international levels.[4] The technical specification[5] published by the International Organization for Standardization (ISO) for heat-flux meters in fire tests addresses calibration levels up to 100 $kW \cdot m^{-2}$ with a combined expanded uncertainty of less than $\pm 3\%$ ($k = 2$). The heat-flux meters used in aerospace applications operate at even higher heat-flux levels. The objective of this paper is to address the radiative calibration of meters at such high-heat-flux levels, which requires resolving additional issues not present when calibrating at low-heat-flux levels.

Two popular type of heat-flux meters are the Gardon and Schmidt–Boelter designs. These meters measure total heat flux because they are sensitive to both radiative and convection contributions. For applications involving predominantly radiative heat flux, the sensing surface is coated with a black paint having high absorptance. The Gardon[6] heat-flux meter consists of a constantan circular foil connected to a copper heat sink at the outer edge. The incident heat flux flows radially outward from the foil center to the heat sink, resulting in a parabolic distribution of the temperature across the foil. The instrument works like a differential thermocouple with the output proportional to the incident total heat flux normal to the foil surface. The Schmidt–Boelter meter (see Ref. 7) is based on a thermopile. The heat flows axially through the sensing surface, and

the temperature distribution across the sensing surface is uniform. The thermopile output is proportional to the temperature difference across a thin, thermally insulating layer and is a measure of the incident total heat-flux.

The calibration of heat-flux meters at the National Institute of Standards and Technology (NIST) employs blackbodies as radiant sources.[8,9] The blackbody temperature and the location of the meter to be tested from the blackbody aperture determine the upper limit on the incident heat-flux level. Conventional calibration with the heat-flux meter located away from the blackbody aperture usually covers only a fraction of the meter's design range. The Swedish technique,[4,10] NT FIRE 050, uses a cooled enclosure attached to the aperture of a spherical blackbody to house the heat-flux meter to be calibrated. The cooled enclosure minimizes the convection contributions to the calibration. The maximum calibration range is approximately 70 $kW \cdot m^{-2}$.

The blackbody temperature and the solid angle subtended at the heat-flux meter by the radiating aperture determine the incident radiant heat flux at the meter. For a given blackbody operating temperature, the radiant heat-flux level at the meter is highest when the solid angle is hemispherical, that is, when the meter is located at the radiating aperture or inside the radiating cavity. This technique, referred to as an in-cavity calibration, has the simplicity in that the incident radiant heat flux derives directly from the Stefan–Boltzmann expression for blackbody radiation.

Two types of blackbody cavity shapes, spherical and cylindrical, are in wide use. For in-cavity calibrations in a spherical blackbody,[11] the maximum achievable radiant heat-flux level is approximately 200 $kW \cdot m^{-2}$ limited by the peak operating temperature of 1100°C. Cylindrical-cavity blackbodies made of graphite operate up to 2700°C, providing in-cavity heat-flux levels up to 4400 $kW \cdot m^{-2}$. However, the corresponding cavity diameters are small compared to spherical cavities, thus limiting the calibration to smaller-size meters. In addition to the restriction on meter size, the in-cavity calibration introduces significant radiation heat exchange between the heated cavity walls and the cooler portions of the heat-flux meter body. Cavity-wall surface emissivity and nonuniform temperature distribution decreases the effective emissivity at the meter location from the theoretical limit of unity. Therefore, the calculation of incident radiant heat flux at the sensing surface of the meter requires an accurate determination of the effective emissivity considering contributions from all of the surfaces participating in the radiation exchange.

The practical application of the in-cavity calibration technique using graphite-tube cylindrical cavities has received only limited attention. An earlier study[12] reported tests by rapidly plunging a cooled heat-flux meter close to the center partition of a 25-mm-diam heated cylindrical dual-cavity blackbody. The results suggested the feasibility of the technique, but lacked proof or validation for wide practical application. The present need to calibrate heat-flux meters at high realistic heat-flux levels has renewed interest in the aerospace community in validating the in-cavity technique using graphite-tube cylindrical cavities. Horn and Abdelmessih[13] analyzed a finite element thermal model of a typical graphite-tube dual-cavity blackbody to understand the heat transfer phenomena inside the cavity, critical for accurate calibration of heat-flux meters.

Presently, an effort is in progress at NIST to develop and validate the in-cavity technique for the calibration of sensors at high radiant heat-flux levels. A recent study[14] using a Monte-Carlo simulation (Fig. 1) demonstrated the critical parameters influencing the steady-state in-cavity calibration of heat-flux meters in cylindrical blackbody cavities. The study showed that the optimal location for the meter is at a distance of approximately one cavity radius away from the closed end of the cavity. At this position, the effective emissivity is highest and relatively insensitive to the temperature gradients along the cavity wall. The other influencing factors are relative size of the heat-flux meter body diameter to the cavity diameter and the reflectance of the meter outer surface exposed to the radiant heat flux. Reducing the body diameter or increasing the reflectance resulted in an increased effective emissivity because of an increased number of reflections a ray undergoes before reaching the sensing surface of the meter. The effect of the holder-surface reflectance on the calculated emissivity was small. Most important, the simulation showed that in the region close to the cavity base, the effective emissivity was very sensitive to the meter location and a strong function of the cavity-wall surface emissivity. In addition, the temperature gradient along the cavity wall was a critical factor influencing the calculated effective emissivity.

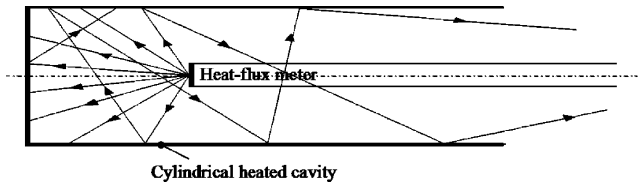

Fig. 1 Heat-flux meter inside heated cylindrical cavity.

Building upon the simulation studies presented in the previous work, the present paper addresses the experimental validation of the in-cavity calibration method using high-temperature, graphite-tube cylindrical cavities. The study uses two different Schmidt-Boelter heat-flux meters tested in two different diameter (25 and 51 mm) cylindrical blackbody cavities. The purpose of testing in the larger 51-mm-diam cavity was to examine the effect of thermal loading, which is difficult to assess accurately from simulation studies. The following sections describe the details of the in-cavity calibration, the associated correction for the emissivity, and a comparison of the in-cavity calibration with the flux-based transfer calibration using the 25-mm-diam blackbody.

II. Facility Description

Figure 2a shows a schematic layout of the 25- and the 51-mm-diam variable-temperature blackbodies (VTBB) used in the present experiments. Both blackbodies have cylindrical cavities, with thermally insulated and electrically heated graphite walls. Direct resistance heating of the cavity walls using large ac at low voltages provides for quick heating and cooling. The heated section of the 25-mm VTBB is 28.2 cm long with a 0.5-cm-thick center partition. A centralized open-loop chilled water supply cools the unit. The water-cooled end caps of the heated graphite tube connect directly to the

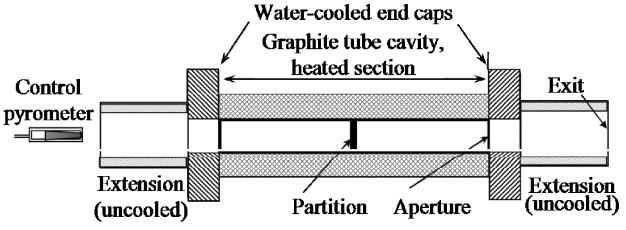

a) Graphite tube blackbody cavity

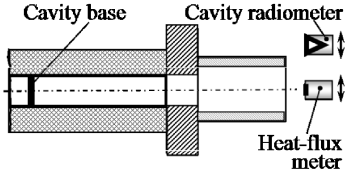

b) Transfer calibration, meter outside cavity

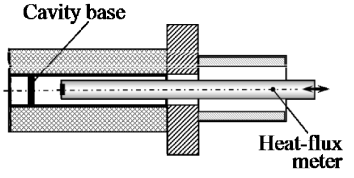

c) In-cavity calibration, meter inside cavity

Fig. 2 Layout of 25- and 51-mm-diam VTBB and heat-flux meter location for calibrations.

heating electrodes. This design aims to provide a sharp temperature gradient between the end cap and the graphite heater element and a uniform temperature distribution along the length of the graphite cavity tube. The maximum operating temperature for the furnace is 2973 K. For routine transfer calibrations up to 50 $kW \cdot m^{-2}$ radiant heat-flux levels, the meter under test and the reference radiometer are placed at a distance of 1.3 cm from the blackbody exit.

The 51-mm-diam VTBB is similar in design to the 25-mm VTBB. The heated section of the blackbody cavity is 48 cm long and has a 0.5-cm-thick center partition. The operating temperature range is from 873 to 2773 K. The time for reaching maximum temperature is about 800 s. Because of large heat dissipation, the cooling system is of closed-loop type consisting of a water-to-water heat exchanger, a circulating pump, and storage and expansion tanks for the water.

The dual-cavity design of the two blackbodies is useful in heat-flux meter calibrations. An optical pyrometer measures the center partition temperature by sensing radiation from one end of the blackbody. A proportional–integral–differential controller regulates the power supply to maintain the furnace temperature to within ± 0.1 K of the set value. The meter under test and the reference radiometer receive radiant heat flux from the other side of the cavity partition. A low-velocity flow of argon gas purges the heated cavities during operation to minimize graphite erosion.

The present experiments consist of the transfer calibration using the 25-mm-diam VTBB with the meter outside the cavity (Fig. 2b) and the in-cavity calibration in both the 25- and 51-mm-diam VTBB, with the meter inserted into the heated cavity (Fig. 2c).

III. Schmidt–Boelter Heat-Flux Meters

The two Schmidt–Boelter (SB) heat-flux meters (Fig. 3) used here are water-cooled and have design total flux ranges of 200 $kW \cdot m^{-2}$ (SB1) and 500 $kW \cdot m^{-2}$ (SB2). The sensor head is mounted at the front end of a 63.5-cm-long, 12.7-mm-diam water-cooled body. The sensing surface has a black coating with an absorptance value of 0.92 over the sensing area. The annular region around the high-absorptance coating is polished copper surface to achieve a high effective emissivity at the sensing surface when placed inside the blackbody cavity. The long stem of the water-cooled body facilitates placing the sensing surface of the meter inside the heated blackbody cavity. The recommended cooling water flow rate is 0.6 l/m. The long stem is made of copper with the outer surface highly polished. A type K thermocouple mounted on the tip of the sensor portion of the meter helps in monitoring the surface temperature rise when exposed to radiant heat flux.

IV. Experimental Results and Discussion

The experimental studies consist of both the outside-cavity transfer calibration covering only a fraction of the heat-flux meter design range and the in-cavity calibration covering the full range. The transfer calibration over the limited range provides baseline responsivity data for comparison with the in-cavity measurements.

A. Transfer Calibration in 25-mm VTBB

The NIST transfer technique[15,16] is currently in use for calibrating heat-flux meters up to 50 $kW \cdot m^{-2}$. The technique uses a room-temperature electrical substitution radiometer (ESR) as a transfer standard. The radiometer calibration is traceable to measurements performed with the high-accuracy cryogenic radiometer (HACR), the U.S. standard for optical power.[17] The heat-flux meter to be calibrated and the transfer standard radiometer, placed a distance of 12.5 mm from the 25-mm VTBB exit, receive equal amount of radiant heat flux from the blackbody cavity. The maximum temperature of the VTBB for these tests is 2533 K. The corresponding view angle subtended at the meter location by the blackbody radiating aperture is approximately 14 deg. Because of the nearly complete absorption of the radiation by the ESR cavity, the ESR measurement gives directly the incident radiant heat flux. This is in contrast to the method of determining the incident heat-flux level based on the blackbody temperature.

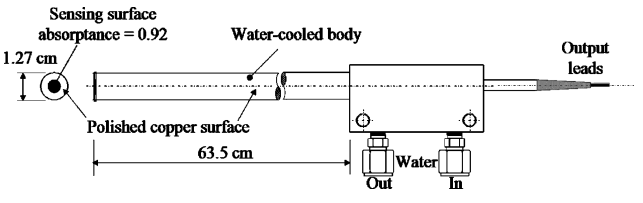

Fig. 3 Schematic of SB1 (200-$kW \cdot m^{-2}$) and SB2 (500-$kW \cdot m^{-2}$) heat-flux meters.

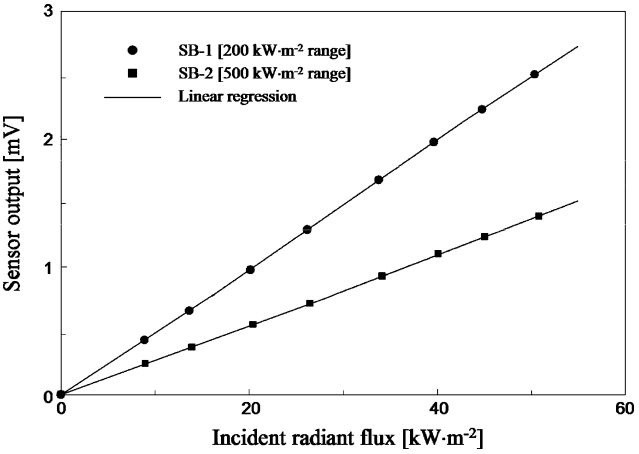

Fig. 4 Flux-based transfer calibration of SB1 and SB2 meters in the 25-mm VTBB.

Figure 4 shows the results of the transfer calibration for the two SB meters. A regression analysis of the data showed that the responses of both of the meters are essentially linear, with correlation coefficients of 1.0000, over the full range of calibration. The calculated responsivity value obtained by linear regression is 0.0510 $mV \cdot kW^{-1} \cdot m^2$ for the lower-range SB1 meter and 0.0283 $mV \cdot kW^{-1} \cdot m^2$ for the higher-range SB2 meter. The relative expanded uncertainty in the responsivity values is 2% ($k = 2$). The direct determination of the heat flux using the ESR provides measurements traceable to national standards and the SI units. The narrow view angle limits the radiant heat-flux level at the meter location to about 50 $kW \cdot m^{-2}$, a fraction of the design range of the meters under test.

B. In-Cavity Tests

The first part of the in-cavity experiments addressed the issues of determining the optimal longitudinal location of the meter within the blackbody cavity and the effect of placing the meter inside the cavity on the blackbody performance. Following these measurements, both the SB1 and SB2 meters were calibrated by insertion into the cavity to the optimal location.

1. Radiance Distribution Inside the Cavity

The measurements covered different locations of the test meter inside the cavity in steps, starting from the end of the heating region and moving gradually toward the cavity base. The positioning at each location was manual. Gradual movement of the meter between different locations ensured stable blackbody operating conditions at the set temperature during the tests. After positioning, the output signal from the heat-flux meter was recorded for 10–15 s.

Inserting a cooled heat-flux meter into the cavity disturbs the thermal equilibrium and the associated empty cavity radiance characteristics. This effect will be larger on the 25-mm VTBB because of its smaller size compared to the larger 51-mm VTBB. Therefore, initial measurements performed in the 25-mm VTBB included the recording of the test meter output at each location along the cavity with a simultaneous recording of the cavity-partition temperature measured by the control pyrometer. The cavity-partition temperature was recorded continuously during a complete cycle of heat-flux meter measurements for different locations inside the

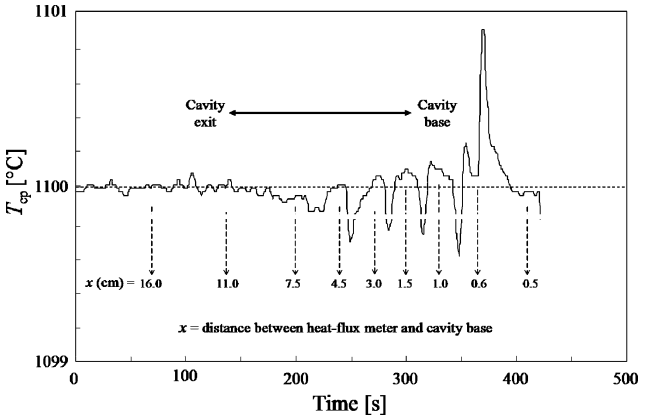

Fig. 5 Typical cavity-partition temperature variation during tests in 25-mm VTBB.

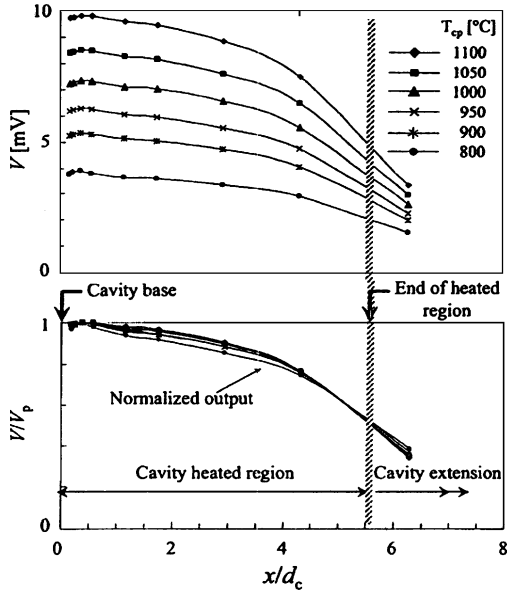

Fig. 6 SB1 heat-flux meter (200-kW/m^2 range) output at various locations inside 25-mm VTBB cavity.

cavity. The blackbody temperature range was from 800 to 1100°C for the lower-range SB1 meter and 800 to 1300°C for the higher-range SB2 meter. Figure 5 shows typical variation of the blackbody cavity-partition temperature over a period of about 500 s when the test meter was placed at various locations inside the cavity. The blackbody set-point temperature was 1100°C.

The change in the blackbody temperature during the test is within ±0.2°C when the cold test meter is away from the cavity base. As the sensing surface of the meter gets closer to the cavity base, the temperature change is higher but still less than ±1 K. However, the blackbody control system corrects for the change to stabilize the temperature within a short time at the set-point value. The spikes in the distribution toward the cavity base correspond to the transients during the test meter movement from one location to the other. Figure 6 shows the corresponding variation in the test meter output as a function of position along the cavity axis as specified by x/d_c. Measurements were made for blackbody temperatures in the range 800–1100°C.

The signal output increases rapidly as the meter is moved from the end of the heating region toward the cavity base indicating increasing levels of incident radiant heat flux. The output reaches a maximum value when the meter is at a distance of about one cavity radius from the base. Further movement of the meter closer to the base decreases the output signal, signifying reduced incident radiant heat flux. The observed trend in the meter output signal variation with position was similar at all temperatures.

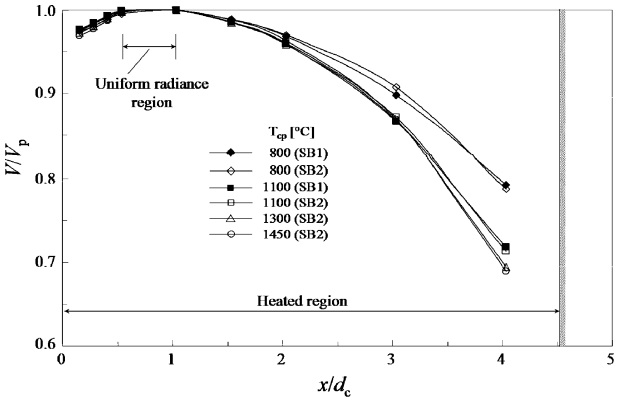

Fig. 7 SB1 and SB2 meters outputs at various locations inside 51-mm-diam VTBB cavity.

The drop in the output voltage when the meter is positioned close to the cavity base demonstrates that the cavity-wall surface emissivity is the dominant factor in determining the incident heat-flux level close to the cavity-base region. Away from the base, because of the larger number of reflections within the cavity, the output signal from the meter should be nearly the same along the length if the temperature distribution along the cavity wall is uniform. However, the output signal after reaching a peak value at $x/d_c \approx 0.5$ decreases significantly when the meter is moved away from the base. This behavior suggests that the cavity-wall temperature distribution is not uniform and is decreasing along the length of the cavity. The drop in the output level is nearly linear in the region from $x/d_c \approx 0.5$ to about $x/d_c \approx 3$. The bottom of Fig. 6 shows the output signal normalized with respect to the peak value, for different blackbody temperatures. At a meter location of $x/d_c \approx 3$, the meter output drops by approximately 12% from the peak value.

The exploratory measurements in the 25-mm VTBB suggest that the optimal meter location inside the cavity is in the region of $x/d_c \approx 0.5$. Away from this location, either the cavity-wall surface emissivity, or temperature distribution, or both affect the incident radiant heat flux and consequently the output signal from the meter. Figure 7 shows similar measurements performed in the 51-mm VTBB using both the SB1 and SB2 meters, for blackbody temperature from 800 to 1450°C. The blackbody radiant heat flux at the higher temperature was approximately 500 kW · m^{-2}, the design limit of the SB2 meter.

In contrast to the 25 mm VTBB measurements, the region of uniform radiance extends from about $x/d_c \approx 0.5$ to $x/d_c \approx 1.0$. The decrease in the output signal is more pronounced for positions closer to the cavity base signifying reduced incident heat flux, compared to the 25-mm VTBB tests (Fig. 6). The output signal distribution of the both the SB1 and SB2 meters in the two blackbody cavities validates the Monte Carlo simulation prediction[14] that the measurement location should be at least one cavity radius away from the base. However, the length of nearly uniform radiance region along the cavity axis depends on the radiating properties of the cavity walls and needs to be experimentally determined for a particular cavity and heat-flux meter combination.

The in-cavity calibration requires calculation of the incident radiant heat flux at the active sensing region of the meter. Both the cavity wall and the test meter's exposed surface participate in the radiant exchange contributing to the incident radiant heat-flux level at the meter's active area. The active sensing area of the meter receives radiant heat flux over the full hemispherical field of view. The assumption of unity emissivity, used in calibrations to calculate the incident heat flux for meters mounted outside the cavity, is not valid for meter locations inside the cavity. In addition to the surface emissivity of the cavity walls, other factors also influence the effective emissivity at the meter position. Practical blackbody cavity walls can have, or develop with time, nonuniform temperature distributions. The effectiveness of the thermal insulation and water cooling can change over time, leading to degradation in the blackbody performance. Furthermore, the cool meter inside the cavity

influences the radiating environment by introducing thermal loading of the cavity. The cooling effect of the meter on the heated cavity can play a major role at high blackbody temperatures, particularly when the meter and cavity dimensions are comparable. All of these factors tend to reduce the effective emissivity from the ideal value of unity. However, the magnitude of the effective emissivity is highest in the region $x/d_c \approx 0.5$ and is relatively uninfluenced by the other extraneous factors.[14]

The measurements during these tests were performed under nearly steady cavity thermal conditions because of the ability of the graphite heating element to adjust quickly to the changing conditions. Figure 8 shows the SB2 meter output with time in the 51-mm VTBB for different operating temperatures. The different rise rates observed in the output signal reflect variations in the manual positioning of the meter inside the cavity. When the active region of the meter is located in the peak radiance region inside the cavity, the output after reaching a maximum gradually decreases with time due to the cooling effect of the water-cooled test meter. The change in output voltage from the peak value was approximately -0.1% at 800°C and -0.3% at 1450°C over a period of 15 s. The corresponding changes in the 25-mm VTBB were larger because of the lower thermal capacity of the cavity: -0.3% at 800°C and -0.8% at 1300°C, limiting the maximum calibration temperature to 1300°C for the 25-mm VTBB tests.

2. Responsivity Measurements

Figure 9 shows the calibration results of the two test meters in the 25- and the 51-mm VTBB. The results show the measured output voltage of the test meters against the calculated blackbody radiant heat flux using the Stefan–Boltzmann equation, assuming an effective emissivity of unity. For the SB1 meter, the calibrations covered the full range of the meter for both blackbody cavities. For the SB2 meter, the tests in the 51-mm VTBB covered the full range of 500 $kW \cdot m^{-2}$, whereas the 25-mm VTBB test was limited to 350 $kW \cdot m^{-2}$ to minimize the effect of thermal loading on the cavity.

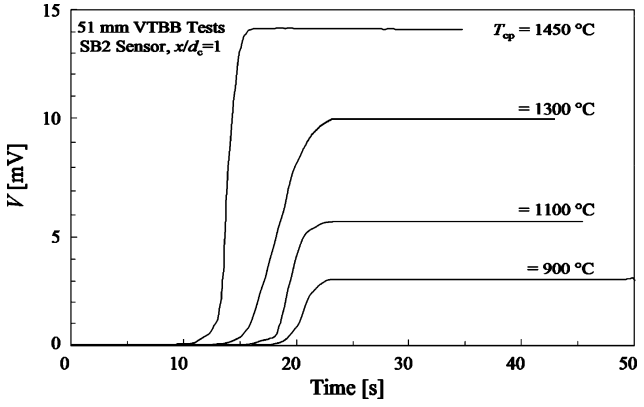

Fig. 8 SB2 heat-flux meter output with time in 51-mm VTBB.

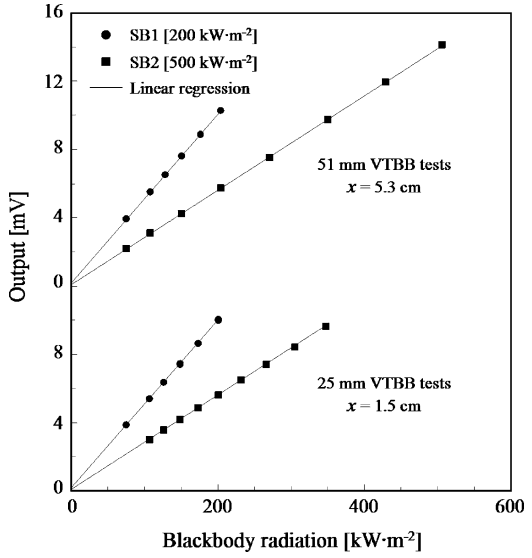

Fig. 9 In-cavity responsivity measurements of SB1 and SB2 heat-flux meters.

Over the radiant heat-flux range in the present measurements, the meter output response is linear with increasing blackbody radiation. A regression analysis shows correlation coefficients of 0.9999 for the 25-mm VTBB and 1.0000 for the 51-mm VTBB test data. The responsivity value for the SB1 meter obtained by the regression analysis is 0.0489 $mV \cdot kW^{-1} \cdot m^2$ in the 25-mm VTBB and 0.0492 $mV \cdot kW^{-1} \cdot m^2$ in the 51-mm VTBB. For the higher-range SB2 meter, the corresponding responsivity values are 0.0275 $mV \cdot kW^{-1} \cdot m^2$ and 0.0276 $mV \cdot kW^{-1} \cdot m^2$ in the 25- and 51-mm VTBB, respectively. The measured responsivity from the two tests in different blackbody cavities differ by about 0.6 and 0.4% for the SB1 and SB2 meters, respectively.

In contrast to the transfer calibration (Fig. 4), the linear regression analysis of the in-cavity data shows a small nonzero intercept at a zero radiant heat-flux level. This intercept is attributed to heat flux arising from nonradiative effects. These effects can be very pronounced and is a major problem when calibrating at low-heat-flux levels. Convection heat transfer, in particular, can be a significant portion of the total flux causing nonlinearity of the meter response when plotted against the calculated radiant heat flux. However, at high-heat-flux levels, as in the present case, the effect of nonradiant heat transfer contributions on the responsivity represented by the slope of curve is small. The radiative heat-flux increase is proportional T^4 and is dominant at high temperatures compared to the convective heat flux, which increases linearly with T. The high degree of linearity of the data suggests that the influence of nonradiant contributions to the heattransfer at the meter remains nearly the same when the radiant heatflux is varied from the lowest heat-flux level of 75 $kW \cdot m^{-2}$ at 800°C to the highest heat-flux level of 500 $kW \cdot m^{-2}$ at 1450°C. Therefore, the slope calculated by the linear regression is a reliable indicator of the meter responsivity to the radiant heat-flux.

3. Correction for the Effective Emissivity

The responsivity determination of the test meters presented in the preceding section assumed blackbody radiant heat flux at the meter location. However, the actual radiant heat flux at the location will be different because the effective emissivity will be lower than the unity value assumed. Our previous paper[14] presents in detail the application of the Monte Carlo method to evaluate the effective emissivity and the associated correction for in-cavity test data. This section summarizes the results of the Monte Carlo calculations using the STEEP3 software[18] for the current experiments.

The factors that affect the effective emissivity are the cavity geometry with the meter in place, the radiative properties of different surfaces, and the cavity-wall temperature distribution. Figure 10 shows the cavity/meter geometry for the 25- and 51-mm-diam cavities. The ratios of the heated length to the diameter of the cavity

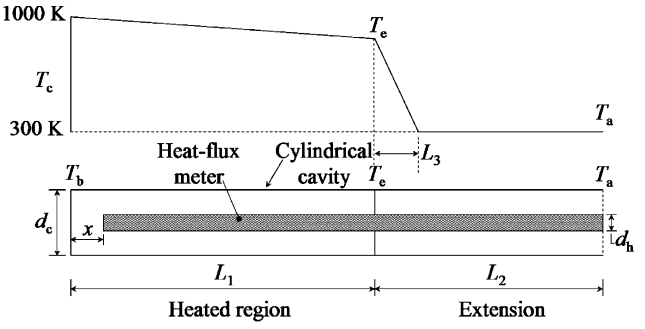

Fig. 10 Computational model of cavity and test heat-flux meter combination for Monte Carlo calculations; 25-mm VTBB: $L_1/d_c = 5.00$, $L_2/d_c = 4.64$, and $d_h/d_c = 0.50$; 51-mm VTBB: $L_1/d_c = 4.00$, $L_2/d_c = 3.43$, and $d_h/d_c = 0.25$.

(L_1/d_c) and the ratio of the cavity extension length to cavity diameter (L_2/d_c) are approximately one diameter shorter for the 51-mm VTBB than for the 25-mm VTBB. The corresponding values for the test meter body to cavity diameter ratio (d_h/d_c) are 0.25 and 0.50, respectively. The distance x from the cavity base to the active area of the meter is variable.

The surface emissivity of the graphite forming the cavity wall depends on the grade of the material and can exhibit a strong spectral dependence. Measurements on samples show the normal total emissivity for the 51-mm VTBB graphite decreases from about 0.83 in the visible region to about 0.73 at 18 μm. For the 25-mm VTBB graphite material, which uses a denser grade of graphite, the emissivity is about 0.88 in the visible region and about 0.85 at 5 μm and longer wavelengths. Because of multiple reflections inside the cavity, the spectral radiance variations have little effect on the total effective emissivity. Therefore, three nominal surface emissivity values of $\varepsilon_c = 0.80$, 0.85, and 0.90 were chosen for the calculations. The absorptance value of the black paint covering the sensing surface of the meter, corresponding to the central portion of the meter front surface (Fig. 3), was $\varepsilon_s = 0.92$. The annular region surrounding the sensing area and the holder surface was a highly polished copper surface with a reflectance value of $\rho_h \approx 0.9$.

The output signal distribution of the two meters shown in Figs. 6 and 7 suggest that temperature is decreasing along the length of the cavity walls of both of the blackbodies. The actual temperature distribution with the meter placed inside the cavity is difficult to measure or to calculate. However, the effective emissivity calculations assuming different temperature distributions along the wall can serve as a guide. A close match between the calculated effective emissivity and the normalized distributions of the output signal is a measure of the possible temperature variation existing along the cavity walls.

The control pyrometer of the blackbody maintains the temperature at the set value by measuring the cavity central-partition temperature. Therefore, it is reasonable to expect that the temperature distribution in the region of the cavity base to be uniform at the set value. For calculation purposes, the cavity-base temperature T_b was set uniform at 1000 K. The distribution from the cavity base to the end of the heating region, T_e, was uniform at 1000 K for isothermal cavity conditions and allowed to decrease linearly to $T_e = 980$, 960, 940, 920, and 900 K to represent possible temperature gradients. The distribution over the graphite extension was set at an ambient value of $T_a = 300$ K, with a linear change in temperature from T_e to T_a over a short distance beginning from the end of the heating region. Figure 11 summarizes the results of the effective emissivity calculations for two locations of the test meter in the blackbodies, $x/d_c = 0.5$ and 4.0, with the assumed temperature distributions for varying T_e.

The evaluation of ε_{eff} uses the cavity-base temperature T_b as a reference. The maximum drop in ε_{eff} from the ideal value of unity at $x/d_c = 0.5$ is about 2% over the entire range of x considered. For $x/d_c = 4.0$, the change is not significant for a uniform temperature distribution of 1000 K. However, ε_{eff} decreases significantly with lowering of the temperature T_e at the end of the heating region. The drop in ε_{eff} for $T_e = 900$ K nearly matches the change in the measured output of the meters at this location. The calculated value of $\varepsilon_{\text{eff}} = 0.984$ (± 0.003) at location $x/d_c \approx 0.5$ is the same for both blackbodies. Therefore, the incident radiant heat flux at this location will be lower by approximately 1.6% compared to the blackbody radiation value. The corresponding correction factor for the measured responsivity values is equal to $(1/\varepsilon_{\text{eff}})$.

The relatively high value of ε_{eff} for both blackbodies is due to the reflecting annular region around the active sensing area covered with high-absorptance paint on the front surface of the meter. The effectiveness of the reflective region is particularly large when the meter is close to the cavity bottom. The cavity-wall temperature gradient also has a significant influence on the effective emissivity.

4. Measurement Uncertainty

Taylor and Kuyatt[19] present the procedure for evaluating the uncertainty in NIST measurements based on the ISO guide.[20] Table 1 gives the standard uncertainties in the various test variables and the corresponding relative expanded uncertainties in the measured responsivity. The expanded uncertainties, obtained by multiplying the standard uncertainties by a coverage factor k, represent the interval within which the measurement result is expected to fall. A value of $k = 2$ corresponds to a confidence level of 95%. The individual uncertainty components are of type A or type B. The standard deviation calculated from random measurements of a variable belongs to a type A uncertainty. Type B (systematic or bias type) uncertainties refer to quantities derived from other means, such as previous experimental data, data from other sources, and calculations using assumed probability distributions. The combined uncertainty,

Table 1 In-cavity calibration of heat-flux meters; measurement uncertainty in responsivity

Uncertainty component (type)	25-mm VTBB tests		51-mm VTBB tests	
	U	U $(k=2)$, %	U	U $(k=2)$, %
Blackbody temperature (B), °C	0.5	0.4	1.1	0.6
Heat-flux meter output, lateral alignment (A), mV	0.04	0.6	——	0.6
Longitudinal alignment (B), mm	0.5	0.6	0.5	0.2
Heat-flux meter reading (A), %	0.1	0.2	0.1	0.2
Effective emissivity evaluation (B)	0.003	0.6	0.003	0.6
Convection heat-flux effects (B), $\text{kW} \cdot \text{m}^{-2}$	3	1.4	3	1.4
Long term repeatability (B), %	0.7	1.4	0.7	1.4
Combined relative expanded uncertainty		2.3		2.2

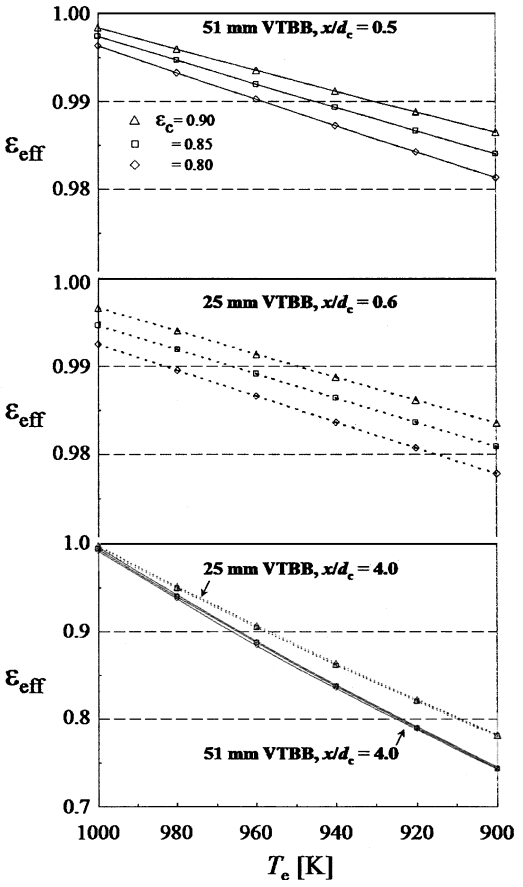

Fig. 11 Monte Carlo calculation results for two locations of heat-flux meter inside cavity.

representing the standard deviation in the responsivity, is the square root of the sum-of-the-squares of the individual uncertainties.

The 25-mm VTBB is a primary facility for all NIST optical pyrometer calibrations. The blackbody temperature measured by the VTBB pyrometer is stable to within ±0.1 K. However, inserting the heat-flux meter in to the cavity affects the cavity temperature. For the experimental conditions in the present test, the change in temperature was within ±0.5 K leading to a maximum uncertainty of 0.2% in the calculated radiant heat flux at 800°C. The calibration of the 51-mm VTBB pyrometer is traceable to radiance temperature calibrations[21] with the 25-mm VTBB. The larger size of the 51-mm VTBB and associated thermal mass helps in maintaining thermal equilibrium during measurement at higher temperatures with the cooler meter inside the cavity. However, the temperature measured by two different pyrometers alternatively looking at either side of the cavity partition differed by 0.1 K at 800°C and 1.1 at 1450°C. The corresponding maximum uncertainty in the calculated radiant heat flux and derived responsivity is 0.3%.

The uncertainty due to lateral positioning of the heat-flux meter inside the cavity was determined in the 51-mm VTBB tests at the highest temperature of 1450°C. The uncertainty in the heat-flux meter (SB2) output, measured at three lateral locations, cavity center and 2.5 mm on either side, was about 0.04 mV, which corresponds to 0.3% standard uncertainty in the responsivity value. This value of uncertainty is assumed for the 25-mm VTBB tests also.

The uncertainty due to longitudinal location of the heat-flux meter on the cavity axis for the 51-mm VTBB test data is small because of nearly uniform distribution in the region $x/d_c = 0.5$–1.0. The 25-mm VTBB data show a peak near $x/d_c = 0.5$, and the meter output decreases on either side. Assuming an uncertainty of 0.5 mm in the meter location away from the peak value position contributes a standard uncertainty of 0.3% to the responsivity.

The output signals from the two meters were steady during measurement interval of about 10–15 s with a calculated standard uncertainty in the output of <0.1%.

Two other components of uncertainty are in determining the effective emissivity and the effect of nonradiant heat flux on the test meter output. As discussed in the preceding section, the uncertainty in the calculated effective emissivity is 0.3% due to possible variations in the input parameter values.

Because the measurements are under ambient conditions, and not under vacuum, convection heat transfer at the sensing surface influences the output from the meter. The test meter and the cavity form an enclosure. Accurate prediction of convection effects inside such an enclosure is complex. The intercepts observed in the linear regression analysis of the experimental data are indicative of the magnitude of the effect of convective heat transfer. Fortuitously, the high degree of linearity of the meter output suggests that the convection heat transfer remains nearly constant over the range of calibration from 70 to 500 $\mathrm{kW \cdot m^{-2}}$. The measured responsivity values differ by only 0.6 and 0.4% for the 25- and 51-mm VTBB test data for the two meters. The good agreement suggests that the influence of the nonradiant heatflux on the meter output is not significant. The heat-flux value corresponding to the intercept on the Y axis is 3 $\mathrm{kW \cdot m^{-2}}$ for both SB1 and SB2 meters. The calculated responsivity value will be higher if we assume the convection effect to be absent and perform a linear regression analysis by setting the intercept value to zero. The responsivity values calculated by the two methods represent upper and lower bounds with an uncertainty of 1.4% ($k = 2$) assuming a rectangular probability distribution for the lower-range SB1 meter. For the SB2, the corresponding uncertainty is lower. However, as a conservative estimate, the same uncertainty value is assumed for both the meters.

Short-term repeat tests in the 51-mm VTBB on the higher-range SB2 meter agreed within 0.1% for the responsivity. The long-term repeatability of the test procedure needs to be established. However, experience with the transfer calibration on a reference SB meter has demonstrated a standard deviation of 0.7% of the responsivity about the mean value over a period last 8 years. This standard deviation provides an estimate for the long-term repeatability.

The corresponding combined relative expanded uncertainties in the heat-flux meter responsivity, for a coverage factor of $k = 2$, are 2.1 and 2.0% for the 25- and 51-mm VTBB tests, respectively.

5. *Responsivity Comparison and Traceability*

Table 2 summarizes the responsivity of the two meters measured by transfer and in-cavity methods. The in-cavity responsivity values measured in the 25- and 51 mm VTBB differ by 0.6 and 0.3% for the SB1 and SB2 meters, respectively. In comparison with the flux-based transfer calibration, the in-cavity responsivity values corrected for effective emissivity are lower by −2.7 and −2.0% for the low-range SB1 meter and by −1.4 and −0.8% for the high-range SB2 meter.

An estimate of the correction to measured responsivity for convection effects is possible by performing the regression analysis with the intercept value set to zero. The average of the two responsivity values, with and without intercept set to zero, represents the best estimate with an associated uncertainty discussed earlier. This correction is approximately 0.0006 and 0.0002 $\mathrm{mV \cdot kW^{-1} \cdot m^2}$ for the SB1 and SB2 meters, respectively. The last line of Table 2 shows the responsivity value accounting for the convection effects to the effective emissivity corrected value. Convection correction results in a much better agreement with the transfer calibration. However, the differences are within the calculated measurement uncertainty limits of 2.3% for both calibration methods. The good agreement between the two methods of calibration tied to national radiant flux (HACR) and temperature standards validates the in-cavity calibration method for high-heat-flux ranges.

We have considered the convection effects based on an analysis of the experimental data. Computational fluid dynamics tools afford a better evaluation of the possible convection effects particularly when calibrating at lower-heat-flux levels. However, the validity of such a code needs checking against suitable experiments. Large uncertainties in convective heat-flux calculations can exist due to uncertainty in input data and other assumptions used in the analysis.

For the range of radiant heat flux in the present study, both blackbody cavities appear to give acceptable level of performance in determining the responsivity. However, it is likely that at still higher radiant heat-flux levels, the cold meter may impose severe thermal loading on the smaller 25-mm VTBB cavity. Therefore, the 51-mm

Table 2 Comparison of in-cavity and transfer calibration measured responsivity

	SB1 (200 $\mathrm{kW \cdot m^{-2}}$), $\mathrm{mV \cdot kW^{-1} \cdot m^2}$		SB2 (500 $\mathrm{kW \cdot m^{-2}}$), $\mathrm{mV \cdot kW^{-1} \cdot m^2}$	
Blackbody	25-mm VTBB	51-mm VTBB	25-mm VTBB	51-mm VTBB
Transfer calibration R_x	0.0510	——	0.0283	——
Effective emissivity in-cavity				
Measured R_m	0.0489	0.0492	0.0275	0.0276
Emissivity $\varepsilon_{\mathrm{eff}}$	0.984	0.984	0.984	0.984
Corrected R_{eff}	0.0496	0.0500	0.0279	0.0281
Difference $(R_{\mathrm{eff}} - R_x)/R_x$, %	−2.7	−2.0	−1.4	−0.8
Convection correction				
Correction to R_{eff}	0.0006	0.0006	0.0002	0.0002
Corrected responsivity R_{corr}	0.0502	0.0506	0.0281	0.0283
Difference $(R_{\mathrm{corr}} - R_x)/R_x$, %	−1.5	−0.8	−0.7	−0.1

VTBB with its higher thermal mass and a nearly uniform radiance in the region $x/d_c = 0.5$–1.0 is expected to be more suitable for extending the in-cavity technique to much higher-heat-flux levels.

C. Other Issues

The in-cavity technique using cylindrical graphite-tube cavities is not widely accepted, primarily due to the difficulty in properly accounting for the complex heat-transfer process associated with a heat-flux meter inside of a cavity, particular when the meter is close to the cavity base, as in the experiments of Brookley and Llewellyn.[12] Some recent unpublished tests on a limited number of heat-flux meters using both the in-cavity technique and the NIST transfer calibration showed differences in measured responsivity much larger than the associated estimated measurement uncertainties. This situation prompted studies to reevaluate the NIST transfer technique and to examine the feasibility of the in-cavity technique as a radiative calibration tool at high-heat-flux levels. Recently, NIST performed measurements using the transfer technique on a number of heat-flux meters from different organizations to obtain a statistical evaluation of the measured responsivity data.[22] The results of this study and the calibration data obtained from the sponsoring organizations compared favorably for a majority of the heat-flux meters tested, reinforcing confidence in the transfer technique. The present paper establishes that the in-cavity technique is feasible and highly promising as an effective tool for the radiative calibration of heat-flux meters.

The favorable agreement between the two techniques will facilitate wider acceptance and further development of the in-cavity technique, which has potential for calibration at high radiant heat-flux levels limited mainly by the blackbody operating temperature. Despite this encouraging situation, it is necessary to recognize the difference between the two calibration techniques. These factors discussed next require careful consideration when assessing the in-cavity measurement results.

1. *Angular Response*

In the NIST transfer technique, the heat-flux meter receives radiant heat flux close to normal viewing conditions. However, the same meter placed inside the cavity, in the absence of a view restrictor as in the present experiments, receives radiant heat flux over the full hemispherical field of view. For a truly Lambertian meter with a cosine angular response, the responsivity measured by the two techniques should agree. The angular response of the meter depends on the properties of the high-absorptance coating on the sensing surface and on the substrate material. A recent paper[23] presents angular responses of two heat-flux meters (110-kW $\cdot$ m^{-2} range), a Gardon and a SB, using different absorptance coatings. For the SB-type meter with the particular coating used, the ratio of hemispherical to normal absorptance was 0.967.

The in-cavity responsivity values for both the SB1 and SB2 meters are lower than the transfer calibration results, suggesting the angular response effects in the in-cavity measurements. Assuming a correction factor of 0.967 as in Ref. 23 largely accounts for the 2.7% lower responsivity of the SB1 meter obtained in the 25-mm VTBB tests, with only effective emissivity correction. A similar correction for SB2 meter data overestimates the responsivity value compared to the transfer calibration results. However, these differences are marginal compared to experimental uncertainties.

2. *Absorbed Heat Flux*

The heat-flux meter responsivity data presented in this paper refers to the incident heat flux. Dividing the responsivity based on the incident flux by the absorptance of the black coating on the sensing area of the meter gives responsivity based on the absorbed heat flux, which is of interest in many applications. The absorbed heat flux depends on the spectral response of the absorptance coating material and the wavelength range over which the source emits radiation. It is desirable to measure the coating absorptance over the wavelength range of interest and use a weighted average for its value. However, in the absence of such information, the manufacturer-specified absorptance value is often used. It is necessary to include the uncertainty in the absorptance value when determining the relative expanded uncertainty based on the absorbed heat flux.

Two types of high-absorptance black paints are in use. The low-temperature coatings usually have a gray or wavelength-independent absorptance over a wide range from 0.2 to 20 μm. The absorptance of high-temperature paints show dependence on the wavelength of the incident radiation and can vary with the substrate material. However, the variation in the weighted average of the total absorptance based on the blackbody spectral radiation is usually small for blackbody temperatures above 800°C. Often, in the application environment or during secondary calibration, the radiant source is a quartz lamp bank emitting radiation over a limited bandwidth. In such situations, an appropriate correction and associated uncertainty evaluation based on the measured spectral response of the absorptance coating may be necessary.

3. *Coating Configuration*

For the heat-flux meters used in this study, the absorptance coating covers only the sensing area and the surrounding annular region is polished copper having a high reflectance. This design was chosen to obtain a high effective emissivity at the sensing surface when the heat-flux meter is placed inside the cavity. However, some heat-flux meters have full coating on the front sensing surface. Monte Carlo calculations show that the effective emissivity in this case, for a cavity-wall emissivity of 0.8, will be about 1.5% lower than with a polished surface when the sensing surface of the meter is at a distance of about one cavity radius from the base. The calculations for a particular test configuration can be performed using a Monte Carlo code (Ref. 14).

4. *Type of Heat-Flux Meter*

This paper addresses the application of the in-cavity technique using thermopile-type SB heat-flux meters. These calibrated meters serve as primary standards to calibrate other secondary standard thermopile heat-flux meters intended for applications in the near future. The procedure and the analysis presented are also applicable for calibrating Gardon circular-foil meters. However, the parabolic temperature distribution across the foil surface and foil peak temperatures as high as 200°C may require careful consideration in the evaluation of the test data.

V. Conclusions

The experimental study on the calibration of heat-flux meters up to 500 kW $\cdot$ m^{-2} demonstrates the feasibility of the in-cavity technique using high-temperature cylindrical-graphite blackbody cavities. The experiments confirm the results of Monte Carlo simulation that the most desirable location for the meter inside the cavity is about a cavity radius away from the cavity base. The value of the emissivity, which determines the level of incident radiant heat flux at the meter, is highest in this region. For the present test configuration, the calculated effective emissivity value is 1.6% lower than the ideal value of unity. The in-cavity measured responsivity values covering the full design range of the meter, when corrected for the effective emissivity and possible convection effects, show good agreement with the flux-based transfer calibration results obtained over a limited range of the meter. The good agreement between responsivity values measured by the two different calibration methods establishes the equivalence between the temperature and radiant flux standards. Further application of the in-cavity technique to radiant heat-flux levels higher than 500 kW $\cdot$ m^{-2} appears feasible, with the larger 51-mm-diam cavity blackbody more suitable because of reduced thermal loading effects.

References

[1] Sarkos, P. C., Hill, R. G., and Johnson, R. M., "Implementation of Heat Release Measurements as a Regulatory Requirement for Commercial Aircraft Materials," *Fire Calorimetry*, Federal Aviation Administration, Rept. DOT/FAA/CT-95/46, Atlantic City International Airport, New Jersey, July 1995, pp. 173–184.

[2]Pitts, W. M., Murthy, A. V., de Ris, J. L., Filtz, J.-R., Nyård, D., Smith, D., and Wetterlund, I., "Round Robin Study of Total Heat-flux Gauge Calibration," National Inst. of Standards and Technology, NIST Special Publ. 1031, Gaithersburg, MD, Oct. 2004.

[3]Grosshandler, W. L., "Heat-flux Transducer Calibration: Summary of the 2nd Workshop," National Institute of Standards and Technology, Rept. NISTIR 6424, Gaithersburg, MD, Nov. 1999.

[4]Persson, B., and Wetterlund, I., "Tentative Guidelines for Calibration of and Use of Heat-flux Meters," Swedish National Testing and Research Inst., SP Rept. 1997:33, Boras, Sweden, 1997.

[5]"Fire Tests—Calibration and Use of Heat-flux Meters—Part 1: General Principles," Rept. ISO/TS 14934-1, International Organization for Standardization, Geneva, 2002.

[6]Gardon, R., "An Instrument for the Direct Measurement of Intense Thermal Radiation," *Review of Scientific Instruments*, Vol. 24, No. 5, 1953, pp. 366–370.

[7]Kidd, C. T., and Nelson, C. G., "How the Schmidt–Boelter Gage Really Works," *Proceedings of the 41st International Instrumentation Symposium*, Instrumentation, Systems, and Automation Society, Research Triangle Park, NC, 1995, pp. 347–368.

[8]Murthy, A. V., Tsai, B. K., and Saunders, R. D., "High Heat-Flux Sensors Calibration Using Blackbody Radiation," *Metrologia*, Vol. 35, No. 4, 1998, pp. 501–504.

[9]Murthy, A. V., Tsai, B. K., and Saunders, R. D., "NIST Radiative Heat-Flux Sensor Calibration Facilities and Techniques," *Journal of Research of the National Institute of Standards and Technology*, Vol. 105, No. 2, 2000, pp. 293–305.

[10]Olsson, S., "Calibration of Radiant Heat-Flux Meters—The Development of a Water-Cooled Aperture for Use with Blackbody Cavities," Swedish National Testing and Research Inst., SP Rept. 1991:58, Boras, Sweden, 1991.

[11]Murthy, A. V., Tsai, B. K., and Saunders, R. D., "Calibration of a Heat-Flux Sensor up to 200 kW/m^2 in a Spherical Blackbody," *Symposium on Thermal Measurements: The Foundation of Fire Standards*, edited by L. A. Gritzo, and N. Alvares, ASTM STP 1427, American Society for Testing and Materials International, West Conshohocken, PA, 2003, pp. 51–66.

[12]Brookley, C. E., and Llewellyn, W. E., "Determination of Blackbody Radiance at Temperatures Above 2300°C," *Temperature: Its Measurement and Control in Science and Industry*, edited by J. F. Schooley, Vol. 6, American Inst. of Physics, New York, 1992, pp. 1195–1199.

[13]Horn, T. E., and Abdelmessih, A. N., "Experimental and Numerical Characterization of a Steady-State Cylindrical Blackbody Cavity at 1100 Degrees Celsius," NASA TM 2000-209022, Aug. 2002.

[14]Murthy, A. V., Prokhorov, A. V., and DeWitt, D. P., "High Heat-Flux Sensor Calibration—A Monte Carlo Modeling," *Journal of Thermophysics and Heat Transfer*, Vol. 18, No. 3, 2004, pp. 333–344.

[15]Murthy, A. V., Tsai, B. K., "Transfer Calibration of Heat-Flux Sensors at NIST," ASME HTD-Vol. 345, *Proceedings of the 32nd National Heat Transfer Conference*, Vol. 7, American Society of Mechanical Engineers, New York, 1997, pp. 81–88.

[16]Tsai, B. K., Gibson, C. E., Murthy, A. V., Early, E. A., DeWitt, D. P., and Saunders, R. D., "Heat-Flux Sensor Calibration," National Inst. of Standards and Technology, NIST Special Publ. 250-65, Gaithersburg, MD, May 2004.

[17]Gentile, T. R., Houston, J. M., Hardis, J. E., Cromer, C. L., and Parr, A. C., "The NIST High Accuracy Cryogenic Radiometer," *Applied Optics*, Vol. 35, No. 7, 1996, pp. 1056–1068.

[18]STEEP3, Ver. 1.3. User's Guide, Virial, Inc., New York, 2000.

[19]Taylor, B. N., and Kuyatt, C. E., "Guidelines for Evaluating and Expressing Uncertainty on NIST Measurement Results," National Inst. of Standards and Technology, NIST Technical Note 1297, Gaithersburg, MD, 1994.

[20]"Guide to the Expression of Uncertainty in Measurement," International Organization for Standardization, Geneva, 1993.

[21]Gibson, C. E., Tsai, B. K., and Parr, A. C., "Radiance Temperature Calibrations," National Inst. of Standards and Technology, NIST Special Publ. 250-43, Gaithersburg, MD, Jan. 1998.

[22]Murthy, A. V., Fraser, G. T., and DeWitt, D. P., "A Summary of Heat-Flux Sensor Calibration Data," *Journal of Research of the National Institute of Standards and Technology*, Vol. 110, No. 2, 2005, pp. 97–100.

[23]Alpert, R. L., Orloff, L., and De Ris, J. L., "Angular Sensitivity of Heat-Flux Gauges," *Symposium on Thermal Measurements: The Foundation of Fire Standards*, edited by L. A. Gritzo and N. Alvares, ASTM STP 1427, American Society for Testing and Materials International, West Conshohocken, PA, 2003, pp. 67–80.